

Combined Ground Penetrating Radar and Seismic System for Detecting Tunnels

Waymond R. Scott, Jr.^a, Tegan Counts^a, Gregg D. Larson^b, Ali C. Gurbuz^a, and James H. McClellan^a

^aSchool of Electrical and Computer Engineering

^bSchool of Mechanical Engineering

Georgia Institute of Technology

Atlanta, Georgia 30332-0250

waymond.scott@ece.gatech.edu

Abstract— An experimental system to collect co-located ground penetrating radar (GPR) and seismic data was developed to investigate possibilities of using the sensors individually or in a cooperative manner to detect shallow tunnels. These sensors were chosen because they sense very different physical properties. The seismic sensor is sensitive to the differences between the mechanical properties of a tunnel and the soil while the GPR is sensitive to the dielectric properties. Raw and processed data from both sensors are presented.

Keywords— component; Shallow tunnels, ground penetrating radar, GPR, seismic

I. INTRODUCTION

It is unlikely that any single sensor will be able to reliably detect tunnels with a reasonable false alarm rate in all environmental conditions. The reason for this is that the soil is a complex, lossy, and very inhomogeneous media. Many of the inhomogeneities in the soil such as layering, moisture variations, rocks, roots, etc. can cause a sensor to give false alarms. The loss in the soil can also be very problematic for certain types of soil. If there is prohibitive attenuation of the waves due to the loss in the soil, the sensors will perform very poorly. It seems reasonable that by using multiple sensors in a coordinated fashion to sense a broad range of physical properties, it will be easier to reliably detect tunnels and distinguish between them and inhomogeneities in the soil.

An experiment to investigate the potential for multiple sensors was set up. In the experiment, co-located ground penetrating radar (GPR) and seismic data were taken. These sensors were chosen because they sense very different physical properties and are compatible with simultaneous operation. The seismic sensor is sensitive to the differences between the mechanical properties of a tunnel and the soil while the GPR is sensitive to the dielectric properties. The loss mechanisms in the soil for the electromagnetic (EM) and the seismic waves are also very different, making it less likely to have prohibitive loss for both wave types in a given soil type.

In the experiments, a scale model for a tunnel was buried in the sandbox at Georgia Tech as in Fig. 1. The GPR uses a multi-static array of modified resistive-vee antennas and operates over the frequency range of 500 MHz to 8 GHz. The

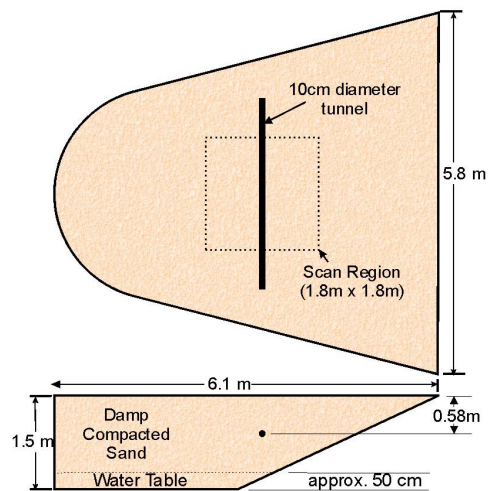


Figure 1. Diagram of the experimental setup.

seismic system is operated in a bi-static mode with an airborne source and a ground contacting receiver and operates over the frequency range of 100 Hz to 8 kHz. Several types of seismic sources and receivers were investigated, but this configuration gave the cleanest received signals.

II. EXPERIMENT

The experimental model, illustrated in Fig. 1, consists of a wedge shaped tank filled with over 50 tons of damp compacted sand to simulate soil. The water table in the sand is approximately 1m deep. A scale model for a tunnel is buried within a 1.8 m x 1.8 m region in the center of the tank. The tunnel is 10cm in diameter and is buried approximately 58 cm deep (the depth varies from 53 to 63 cm), making about a 20 to 1 scale model for a shallow tunnel just big enough for a man to slide through. The sensors are scanned over this region with a three degree-of-freedom positioner. Diagrams of the sensors and photographs of the sensors are shown in Figs. 2 and 3.

This work is supported in part by the U.S. Army Research Office under contract number DAAD19-02-1-0252.

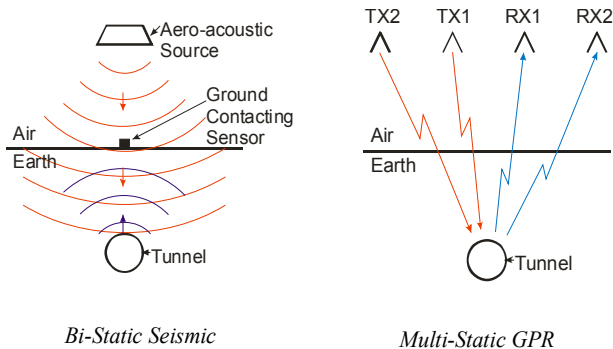


Figure 2. Diagram of the multi-static GPR and the bi-static seismic system.

A. Multi-static GPR

The GPR sensor consists of six resistively-loaded vee antennas arranged to form eight bi-static pairs. These antennas are very “clean” in that they have very little self clutter and a very low radar cross section to lessen the reflections between the ground and the antennas. The antennas have an aperture length of 11.4 cm and are spaced 12 cm apart [1-2]. The response of the antennas is measured with a network analyzer over the frequency range of 60 MHz to 8 GHz. The data is then transformed into the time domain to give the response of the antennas to a differentiated Gaussian pulse with a center frequency of 2.5 GHz. The equivalent pulse for the full size system would have a $2.5 \text{ GHz}/20 = 125 \text{ MHz}$ center frequency.

Images were created from the GPR data using a migration algorithm on each bistatic pair and then coherently summing the images to get the final image [3-4]. The multi-static nature of the system allowed us to use a post-migration move-out to get an accurate estimate for the wave velocity in the sand. Images are shown in Fig. 4 for three planes that pass through the tunnel on a 25 dB scale. A three-dimensional iso-image for a 15 dB surface is shown in Fig. 5b. The tunnel is clearly seen in the images and appears at the approximately the correct depth. The strength of the response to the tunnel is seen to be much stronger for $-60 \text{ cm} < y < 40 \text{ cm}$. One explanation of this is that water has collected in that portion of the tunnel since it is the deepest part. This will be investigated upon excavation of the tunnel. A portion of the sloping tank bottom can also be seen in the images.

B. Seismic Sensor

The seismic sensor consists of an aero-acoustic source and a ground contacting receiver. The acoustic source is a 13 cm speaker with a closed box, and the ground-contacting receiver is an accelerometer that is coupled to the ground with a biasing force provided by a tail mass through a spring. The speaker and accelerometer are scanned across the surface using the positioning system. The speaker is excited with a 4 s chirp with frequency content from 100 Hz to 8 kHz. These data are used to synthesize the response of the system to a differentiated Gaussian pulse with a center frequency of 3.6 kHz. The equivalent pulse for the full size system would have a $3.6 \text{ kHz}/20 = 180 \text{ Hz}$ center frequency.

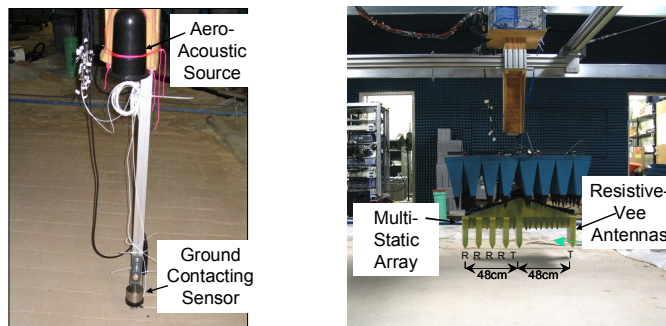


Figure 3. Photographs of the multi-static GPR and bi-static seismic system.

Images were created from the seismic data using a migration algorithm. Images are shown in Fig. 4 for three planes that pass through the tunnel on a 20 dB scale, and a three-dimensional iso-image for an 11 dB surface is shown in Fig. 5a. The tunnel is clearly seen in the images and appears at approximately the correct depth. The resolution of the seismic images is higher than that of the GPR images, which may be surprising since the wavelength at the center frequency is approximately 8 cm for the seismic system and 6 cm for the GPR system. The reason for this is that the loss for the electromagnetic waves traveling in the sand increases dramatically with increasing frequency, effectively low-pass filtering the electromagnetic waves.

The sloping tank bottom is much more apparent in the seismic images than in the GPR images. This is due to the stronger contrast between the mechanical properties of the concrete bottom and the sand than between their electrical properties.

The seismic images are somewhat “noisier” than the GPR images. The increased “noise” is much more apparent in the raw data. The source of this “noise” is not known as it does not appear to be thermal or background seismic noise as it does not occur at times before the excitation pulse.

The seismic and GPR images are somewhat complementary in that the strongest part of the GPR image (at approximately $y = -20 \text{ cm}$) is the weakest part of the seismic image and the weak parts of the GPR image are relatively strong in the seismic image. A three-dimensional iso-image for a 10 dB surface of a combined GPR and seismic image is shown in Fig. 6. This image is somewhat more consistent than either the GPR or seismic image.

III. RADON TRANSFORM FOR DETECTION OF TUNNELS

The Radon transform maps an image into a parameterized domain such that the parameterized shapes (lines and curves) correspond to a peak in the parameter domain. For the specific application of tunnel imaging and detection, we model tunnels as lines over short distances; thus the problem of tunnel detection is converted to a problem of detecting the corresponding peak in the Radon space.

To obtain the depth information of the tunnel as well as the positioning on x and y axis, a 3-dimensional Radon transform of the migrated seismic and GPR data is taken. The line parameterization in 3D and the Radon transform can be found in [5]. Applying the 3D Radon transform to the migrated data and taking the maximum peak in the parameter domain gives the line estimates shown in Figs. 5 and 6.

The sloped part of the sandbox can be seen clearly in seismic image due to mechanical contrast while it is not very clear in GPR image. Despite this, the line estimates pick the tunnel responses in each image correctly. Line estimates from seismic, GPR and combined data are shown together in Fig. 7. The three estimates agree quite well.

IV. CONCLUSIONS

The tunnel is clearly visible in the images from both the GPR and the seismic sensor. The images are somewhat complimentary and combining them resulted in an improved image. The radon transform was shown to be able to extract the location of the tunnel from all three images.

REFERENCES

- [1] Kim, K. and Scott, W.R., Jr., "Design of a Resistively-Loaded Vee Dipole for Ultra-Wideband Ground-Penetrating Radar Applications," *IEEE Trans. on Antennas and Propagation*, Vol. 53, No. 8, August 2005.
- [2] Kim, K. and Scott, W.R., Jr., "Investigation of Resistive Vee Antennas for a Multi-Static Ground-Penetrating Radar," *IEEE Antennas and Propagations Society International Symposium*, Washington, DC, July 3-8, 2005.
- [3] X. Feng and M. Sato, "Pre-stack migration applied to GPR for landmine detection," *Inverse Problems* 20, pp. 99 - 115, 2004.
- [4] E. Johansson and J. Mast, "Three dimensional ground penetrating radar imaging using a synthetic aperture time-domain focusing," *Proc. of SPIE Conference on Advanced Microwave and Millimeter Wave Detectors*, 2275, pp. 205-214, 1994.
- [5] P. Toft, "The Radon Transform Theory and Implementation", Ph.D. Thesis, Technical University of Denmark, Denmark, 1996

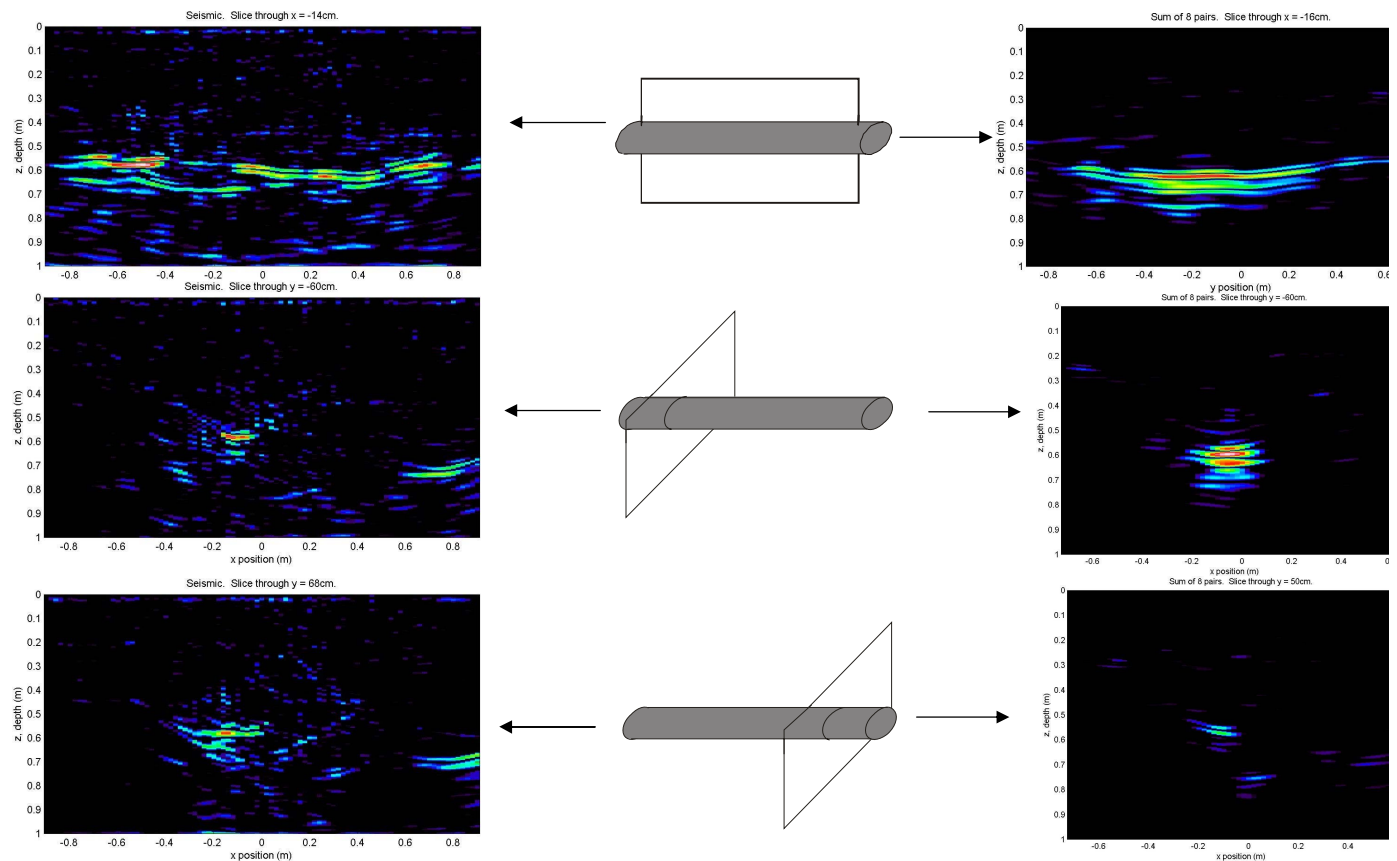
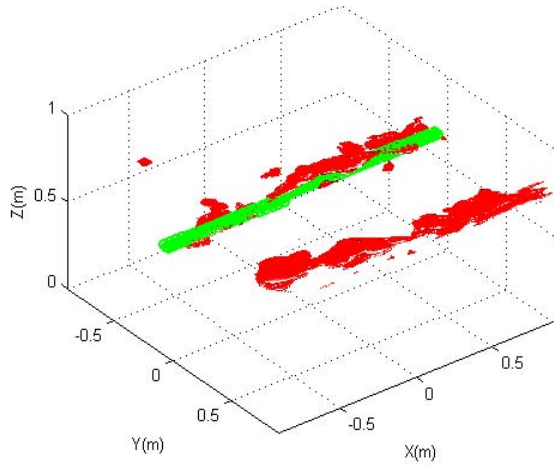
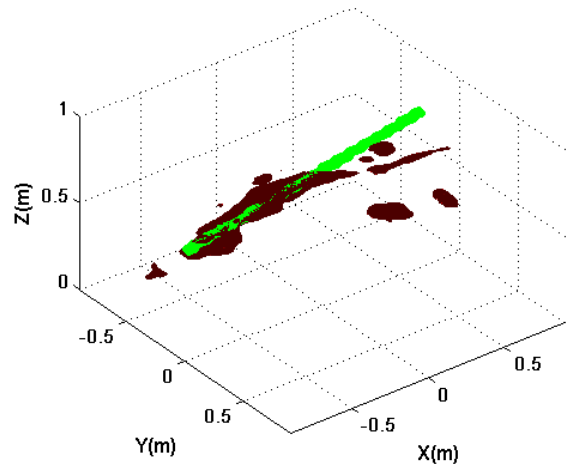


Figure 4. Images formed by a three-dimensional migration of the GPR and seismic data. Pseudo-color graphs are plotted for three planes that pass through the tunnel. The seismic images are on the left and the GPR images are on the right. The seismic images are on a 20 dB scale and the GPR images are on a 25 dB scale.



(a)



(b)

Figure 5. Iso-surface images of the migrated (a) seismic (b) GPR data with line estimates from 3D Radon Transform. The seismic image is a 11 dB iso-surface and the GPR image is a 15 dB iso-surface.

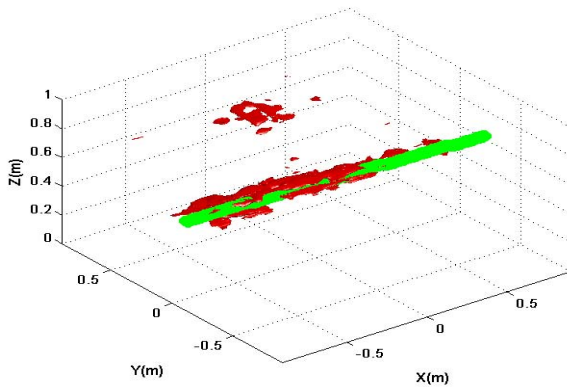


Figure 6. Iso-surface image for combined seismic and GPR data with line estimate from 3D Radon Transform. The image is a 10 dB iso-surface.

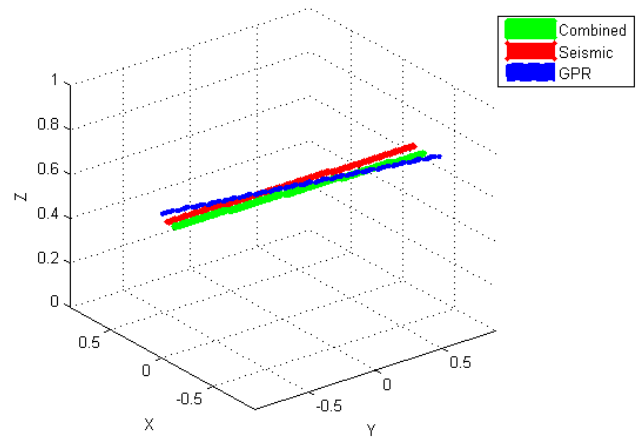


Figure 7. Line estimates for seismic, GPR and combined data sets from 3D Radon Transform.